

Exact gap-ratio results for mixed Wigner surmises of up to 4 eigenvalues

Mikael Fremling

*Institute for Theoretical Physics and Center for Extreme Matter and Emergent Phenomena,
Utrecht University, Princetonplein 5, 3584 CC Utrecht, The Netherlands*

We compute some exact results for the gap-ratio of mixed Wigner surmises for up to four eigenvalues and $0 \leq \beta \leq 4$. The main results concern equal mixtures of the GOE, GUE, and GSE random matrix classes. These give rise to $2 \times \text{GOE}$, $2 \times \text{GUE}$, and $2 \times \text{GSE}$ distributions. We find that $2 \times \text{GOE}$, $2 \times \text{GUE}$ are well approximated by the surmises of only $2+2$ eigenvalues that are GOE and GUE distributed, respectively. The same is not valid for $2 \times \text{GSE}$, which is well estimated, by coincidence, by $2+2$ eigenvalues of statistics intermediate between GUE and GSE.

I. INTRODUCTION

Random matrix theory (RMT) can be used to analyze the spectral statistics of quantum mechanical Hamiltonians. If a Hamiltonian is non-integrable or has a chaotic semiclassical limit, then its distribution of energy levels will generically follow one of the three random matrix ensembles Gaussian-Orthogonal-Ensemble (GOE), Gaussian-Unitary-Ensemble (GUE), or Gaussian-Symplectic-Ensemble (GSE). If the Hamiltonian is integrable, the energy levels appear uncorrelated, resulting in Poisson statistics[1–4].

We can refine the quite generic picture described above by considering Hamiltonians with a single, or a few, unresolved symmetries. An unresolved symmetry is a quantum number that block-diagonalizes the Hamiltonian, but which has not been utilized. As a result, the spectral statistics will break into two (or more) independent ensembles. If the spectrum breaks into two independent GOE, GUE, or GSE ensembles, we call them $2 \times \text{GOE}$, $2 \times \text{GUE}$, and $2 \times \text{GSE}$, respectively. The $2 \times \text{GxE}$ ($x = \text{O, U, S}$) ensembles are not the same as the Poissonian of independent variables, as not all eigenvalues are uncorrelated. For an illustration of this process, see Fig. 1a-b).

Many situations could lead to the $2 \times \text{GxE}$ ensembles listed above, for instance, when there is an unresolved \mathbb{Z}_2 symmetry. In the recent literature, one can find examples in Floquet systems [5–7], the Fractional Quantum Hall Effect [8], restricted SYK models [9–11], and fracton models [12–15].

To study the spectral statistics of a Hamiltonian with (ordered) eigenvalues λ_n , an early method was that of the nearest-neighbor spacing distribution for the variable $s_n = \lambda_n - \lambda_{n-1}$. However, the distance energy spacing depends on the overall energy scale which needs to be divided away. Further, the local density of states could depend on energy, which would be accounted for with a process called unfolding, see Fig. 1c-d)

To circumvent the somewhat arbitrary unfolding procedure, Oganesyan and Huse [16] suggested using the gap-ratio distribution

$$r_n = \frac{s_{n+1}}{s_n} = \frac{\lambda_{n+1} - \lambda_n}{\lambda_n - \lambda_{n-1}},$$

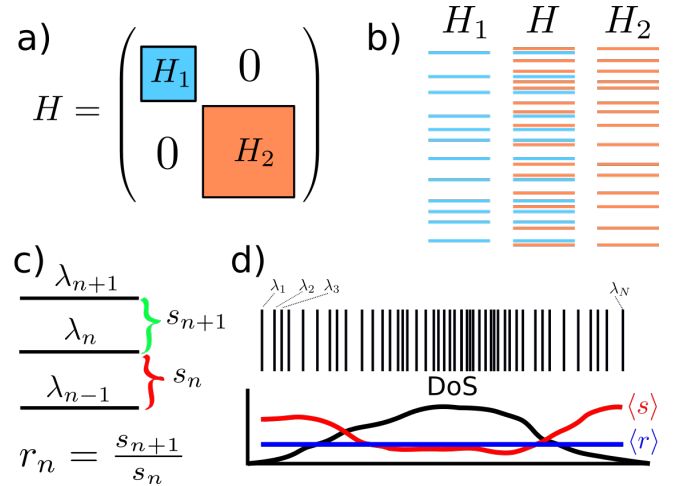


Figure 1. a) If a Hamiltonian, H , contains a symmetry, it can be used to split the Hamiltonian into two (or more) blocks H_1 , H_2 , ... whose spectra are independent. b) The spectra of H_1 and H_2 will show level-repulsion, which is masked in H where the spectra are superimposed. c) Pictorial representation of the level spacing, s , and the gap-ratio, r . d) In a typical Hamiltonian (random matrix), the density of states (DoS) is not constant at all energies. As a consequence, the “local” gap spacing, $\langle s \rangle$, is not constant, which can be remedied by unfolding. On the other hand, the “local” gap-ratio, $\langle r \rangle$, is constant, making it easier to work with it.

since it is invariant under smooth scale changes. In two papers, Atas *et al.* [17, 18] derived a set of analytic results (see Eqn. (5)) regarding the distribution of distribution of r , based on the Wigner surmise for a small number of eigenvalues.

In recent years, a number of generalizations have been added to the literature on higher-order level spacings [19–26] and non-hermitian Hamiltonians [27]. This short paper adds to the current literature by computing exact r -distribution functions for mixed Wigner surmises, such as two superimposed GUE spectra. In passing, we will also collect some lesser-known results from the literature. The work in Ref. 24 also considers level statistics of mixed ensembles, but from a slightly different perspective than the present work.

Computer algebra has been used extensively to minimize clerical errors when deriving the results of this pa-

Distributions	Eqn. no.	$\langle r \rangle$	Distribution	Eqn. no.	$\langle r \rangle$	Distribution	Eqn. no.	$\langle r \rangle$
$P_{1,1}^{2,2}(r)$	(24)	0.422798	$P_{1,0}^{2,1}(r)$	(13)	0.419427	$P_{0,1}^{2,2}(r)$	20	0.403566
$P_{2,2}^{2,2}(r)$	(25)	0.420518	$P_{2,0}^{2,1}(r)$	(14)	0.408545	$P_{0,2}^{2,2}(r)$	21	0.398237
$P_{3,3}^{2,2}(r)$	(26)	0.409623	$P_{3,0}^{2,1}(r)$	(15)	0.404868	$P_{0,3}^{2,2}(r)$	22	0.395907
$P_{4,4}^{2,2}(r)$	(27)	0.39371	$P_{4,0}^{2,1}(r)$	(16)	0.408545	$P_{0,4}^{2,2}(r)$	23	0.395762
Distribution	Eqn. no.	$\langle r \rangle$	$P_0^4(r)$	(12)	0.398237	$P_1^4(r)$	(11)	0.531785
$P_{1,2}^{2,2}(r)$	(28)	0.423367	$P_{2,3}^{2,2}(r)$	31	0.418542	$P_{1,0}^{3,1}(r)$	(17)	0.429718
$P_{1,3}^{2,2}(r)$	29	0.426026	$P_{2,4}^{2,2}(r)$	32	0.420494	$P_{2,0}^{3,1}(r)$	(18)	0.420664
$P_{1,4}^{2,2}(r)$	30	0.431454	$P_{3,4}^{2,2}(r)$	33	0.405069	$P_{3,0}^{3,1}(r)$	(19)	0.40585

Table I. Table of the various mixed Wigner surmises considered in this work, their equation number and expectation value for \tilde{r}_n in Eqn. (2).

per. We use custom-built Julia code that communicates with Mathematica by using the MathLink and MathLinkExtras packages, and the implementation is outlined in Appendix A.

This paper is organized as follows: In Section II we introduce some notation, and recapitulate the result of Atas *et al.* [17]. We also discuss the added complications independent (mixed) Wigner surmises. In section III we perform numerical tests, while the functional form of our analytical results is presented in section IV. As a reference, the main results, and their equation numbers, are summarized in Table I.

II. THE WIGNER SURMISE

In this section we begin by reviewing the approach taken by Ref. 17 to compute the gap-ratio distribution $P_\beta^3(r)$. As starting point we will use the Wigner surmises for the Random Matrix ensembles GxE with $x = O, U, S$, which is known to approximate well the statistics for large random matrices [28]. For N eigenvalues the surmise takes the form

$$P_\beta^N(\lambda) \propto e^{-\sum_{j=1}^N \lambda_j^2} \prod_{i < j=1}^N |\lambda_i - \lambda_j|^\beta \quad (1)$$

where $\beta = 1, 2, 4$ corresponding to $x = O, U, S$. This form is exact for 2×2 matrices and also agrees with the asymptotic distribution [28]. From $P_\beta^N(\lambda)$ one computes the r -statistics by sorting the eigenvalues λ and computing the distribution of

$$r_n = \frac{\lambda_{n+1} - \lambda_n}{\lambda_n - \lambda_{n-1}}.$$

In this work, just like in Ref. 17, we define r on the semi-open interval $r \in [0, \infty)$ rather than the closed interval $\tilde{r} \in [0, 1]$ corresponding to

$$\tilde{r}_n = \min(r_n, 1/r_n) \quad (2)$$

In principle $P(r)$ and $P(\tilde{r})$ could be different, however, if $P(r)$ has the property $P(\frac{1}{r}) = P(r)r^2$ then $P(\tilde{r}) =$

$2P(r)$. This is the case for all distributions considered here.

For $N = 3$ one may, without loss of generality, assume that $-\infty < \lambda_1 < \lambda_2 < \lambda_3 < \infty$ and (1) takes the form of

$$P_\beta^3(\lambda_1, \lambda_2, \lambda_3) \propto e^{-\sum_{n=1}^3 \lambda_n^2} \times (\lambda_2 - \lambda_1)^\beta (\lambda_3 - \lambda_1)^\beta (\lambda_3 - \lambda_2)^\beta. \quad (3)$$

The distribution for r is computed by multiplying with $\delta\left(r - \frac{\lambda_3 - \lambda_2}{\lambda_2 - \lambda_1}\right)$ and performing the nested integrals over $\lambda_1, \lambda_2, \lambda_3$ as

$$P_\beta^3(r) \propto \int_{-\infty}^{\infty} d\lambda_1 \int_{\lambda_1}^{\infty} d\lambda_2 \int_{\lambda_2}^{\infty} d\lambda_3 \times P_\beta^3(\lambda_1, \lambda_2, \lambda_3) \delta\left(r - \frac{\lambda_3 - \lambda_2}{\lambda_2 - \lambda_1}\right) \quad (4)$$

where the delta function $\delta\left(r - \frac{\lambda_3 - \lambda_2}{\lambda_2 - \lambda_1}\right)$ is inserted to ensure that $\int_0^\infty dr P_\beta^3(r) = 1$. The first integral can easily be evaluated to give

$$P_\beta^3(r) \propto (r^2 + r)^\beta \int_{-\infty}^{\infty} d\lambda_1 \int_{\lambda_1}^{\infty} d\lambda_2 \times e^{-\lambda_1^2 - \lambda_2^2 - (\lambda_2 + r(\lambda_2 - \lambda_1))^2} (\lambda_2 - \lambda_1)^{3\beta+1}.$$

Further by rewriting $\lambda_2 = \delta + \lambda_1$ the integral over λ_1 can immediately performed to give

$$P_\beta^3(r) \propto (r^2 + r)^\beta \int_0^\infty d\delta e^{-\frac{2}{3}\delta^2(r^2+r+1)} \delta^{3\beta+1}.$$

The final Gaussian integral is readily evaluated to yield the result

$$P_\beta^3(r) = \frac{1}{Z_\beta} \frac{(r + r^2)^\beta}{(1 + r + r^2)^{1+\beta\frac{3}{2}}}, \quad (5)$$

with Z_β being the normalization constant.

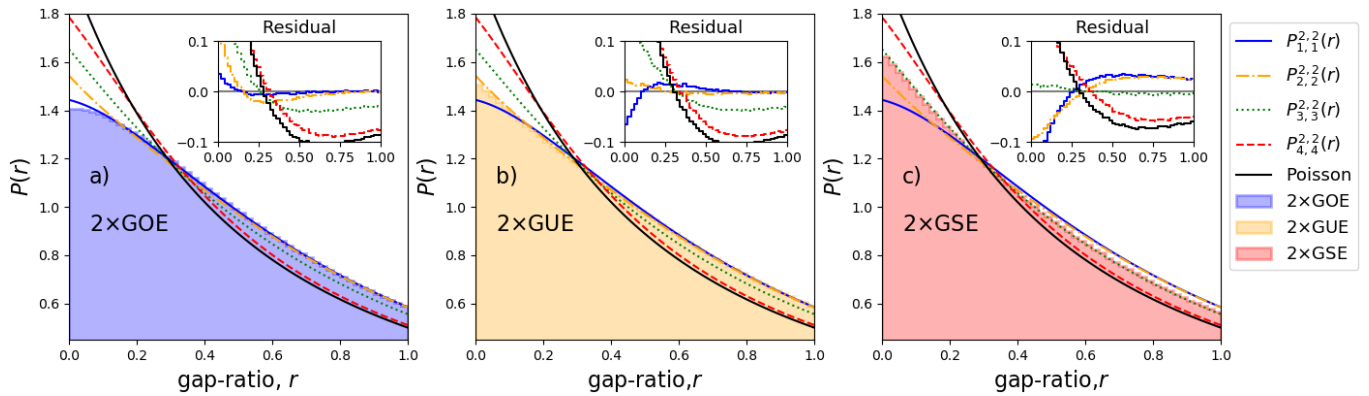


Figure 2. Comparison of the asymptotic $2 \times GxE$ distributions to the analytic $2+2$ surmises $P_{\beta,\beta}^{2,2}(r)$, for $\beta = 1, 2, 3, 4$. The inset shows the residual $P_{\beta,\beta}^{2,2} - P_{2 \times GxE}$. For a) $2 \times GOE$ and b) $2 \times GUE$, the surmises $P_{1,1}^{2,2}$ and $P_{2,2}^{2,2}$ give a good approximation, with some deviation at small r . On the other hand, $2 \times GSE$ is not approximated well with the surmise $P_{4,4}^{2,2}$. However, by coincidence, $P_{3,3}^{2,2}$ gives an excellent surmise for $2 \times GSE$.

A. Mixed Surmises

In this work we will focus on products of Wigner surmises that allow for uncorrelated eigenvalues. Equation (1) is then generalized as

$$P_{\beta}^{\bar{N}}(\lambda) \propto \prod_{\alpha} P_{\beta_{\alpha}}^{N_{\alpha}}(\lambda \in \Lambda_{\alpha}), \quad (6)$$

where Λ_{α} is the set of N_{α} eigenvalues that follow the Wigner surmise with coefficient β_{α} . Distributions of this form are found in the spectrum when there are unresolved symmetries in the Hamiltonian.

Compared with Eqn. (1), there are also two extra levels of complication when computing $P_{\beta}^{\bar{N}}(r)$. The first is that one may not assume that $\lambda_i > \lambda_j$ if i and j come from different sets of eigenvalues. Rather one needs to separately treat all permutations of $N = \sum_{\alpha} N_{\alpha}$ elements divided into groups Λ_{α} of sizes N_{α} . The multi-nomial coefficient

$$M = \frac{N!}{\prod_{\alpha} N_{\alpha}!},$$

then gives the number M of such combinations. Each such permutation comes with a different ordering of the λ s, and they need all be taken into account. Secondly, for a given permutation there are $N - 2$ different gap ratios that contribute to the final distribution $P_{\beta}^{\bar{N}}(r)$.

Thus, for a given ordering σ of the eigenvalues λ , we may define a map $g_j = \lambda_{\sigma(j)}$ to a new set of variables g . This set will have the property that $g_i > g_j$ if (and only if) $i > j$. The generalization of Eq. (4) for M permutations of N eigenvalues then reads

$$P_{\beta}^{\bar{N}}(r) \propto \sum_{\sigma=1}^M \sum_{k=1}^{N-2} P_{k,\sigma}(r).$$

Here, $P_{k,\sigma}(r)$ is the probability distribution for the k 'th gap ratio of the permutation σ , and $k = 1, \dots, N - 2$ enumerates the different gap ratios averaged over. It takes the form

$$P_{k,\sigma}(r) = \int_{-\infty}^{\infty} dg_1 \int_{g_1}^{\infty} dg_2 \dots \int_{g_{N-1}}^{\infty} dg_N \times P_{\sigma}(g) \delta\left(r - \frac{g_{k+2} - g_{k+1}}{g_{k+1} - g_k}\right), \quad (7)$$

where $P_{\sigma}(g) = P_{\beta}^{\bar{N}}(\lambda_{\sigma(j)})$ is the (unnormalized) conditional probability distribution for the permutation σ . Needless to say, the scope for errors in algebraic book-keeping is paramount.

In the present work, we solve both of these combinatorial headaches by automating the integration procedure and using computer-generated Mathematica and Julia code. For a more detailed discussion of the setup, we refer to Appendix A, and in the following section, we merely present the results.

III. COMPARISON TO NUMERICS

To gauge the usefulness of these new distributions, we focus on the $P_{\beta,\beta}^{2,2}(r)$ distributions and compare with numerical results. To obtain the asymptotic $2 \times GxE$ distribution, we constrict two independent Hermitian matrices with random entries and diagonalize them to get their real spectrum. For $\beta = 1$ ($\beta = 2$), the matrices are $N \times N$ with random normal distributed real (complex) numbers. For the GSE case, we use a $2N \times 2N$ dimensional matrix with entries $q = \sum_{j=0}^3 a_j k_j$ where the a_j are normal-distributed. The quaternions k_j are represented by the 2×2 matrices $k_0 = 1_{2 \times 2}$, $k_j = i\sigma_j$, where σ_j are the Pauli matrices. The GSE-spectrum then has an exact two-fold degeneracy that we remove before computing the r -statistics.

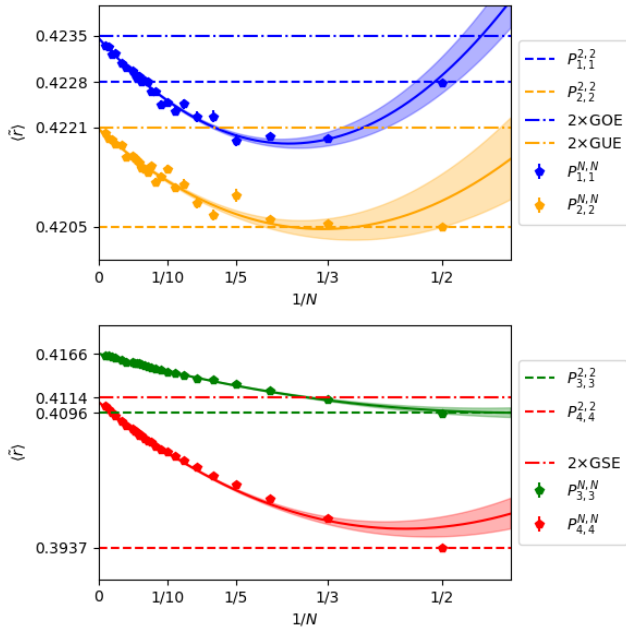


Figure 3. Comparison of $\langle \tilde{r} \rangle$ for $P_{\beta,\beta}^{N,N}$ and $2 \times GxE$ (dash-dotted lines) for a) $\beta = 1, 2$ and b) $\beta = 3, 4$. As a guide to the eye the $P_{\beta,\beta}^{2,2}$ results are shown in dashed lines. In panel a) we find, for $\beta = 1$, that the surmise of $P_{1,1}^{2,2}$ is initially the best approximation of $2 \times GxE$ and is only improved upon at around $N = 15$. For $\beta = 2$ and $\beta = 3$, the improvement seems to be monotonic. It is worth noting that the fit for $2 \times GxE$ by $P_{3,3}^{2,2}$ is only surpassed by $P_{3,3}^{N,N}$ at around $N = 100$. Each data point is computed from 10^6 MC samples, except for $N = 2, 3, 4$ where 10^7 samples were used, to improve accuracy.

In Figure 2 we first compare $P_{\beta,\beta}^{2,2}(r)$ for $\beta = 1, 2, 3, 4$ to the asymptotic distributions obtained numerically. In the figure $P_{1,1}^{2,2}(r)$ and $P_{2,2}^{2,2}(r)$ give a reasonable surmise for $2 \times GxE$ and $2 \times GUE$, respectively. On the other hand $P_{4,4}^{2,2}(r)$ does not give a good approximation for $2 \times GSE$. However, it seems that $P_{3,3}^{2,2}(r)$ does give a good surmise for $2 \times GSE$. We will see below in Fig. 3b that this is a coincidence and that the asymptotic limit of $P_{3,3}^{N,N}(r)$ gives the wrong surmise.

In Figure 3b, the coincidental nature of the good fit for $2 \times GSE$ using $P_{3,3}^{2,2}(r)$ is made more explicit. In the figure, we show $\langle \tilde{r} \rangle$ for $P_{\beta,\beta}^{N,N}$ and compare with $2 \times GxE$ (dash-dotted lines). We use standard Metropolis-Hasting Monte-Carlo sampling to generate the $P_{\beta,\beta}^{N,N}$ distribution and from there compute $\langle \tilde{r} \rangle$. As a guide to the eye, the analytical results of $P_{\beta,\beta}^{2,2}$ are displayed in dashed lines. We see in the figure that the average of $P_{3,3}^{2,2}$ ($\langle \tilde{r} \rangle = 0.4096$, green) by accident comes close to the asymptotic $2 \times GSE$ result ($\langle \tilde{r} \rangle = 0.4114$). However, as N is increased, $P_{3,3}^{N,N}$ overshoots and approaches the much higher average $\langle \tilde{r} \rangle = 0.4166$.

We expect that series of surmises given by $P_{4,4}^{N,N}$ will

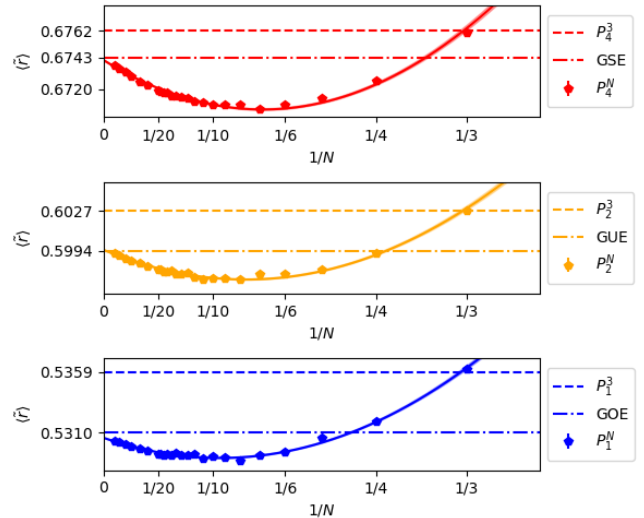


Figure 4. Comparison of $\langle \tilde{r} \rangle$ for P_{β}^N and GxE (dash-dotted lines) for $\beta = 1, 2, 3$. As a guide to the eye, the P_{β}^3 results are shown in dashed lines. In all three panels we find that P_{β}^3 initially overestimates $\langle \tilde{r} \rangle$, and that larger N brings the estimate down to then underestimate $\langle \tilde{r} \rangle$. Finally for $N \gtrsim 100$, P_{β}^N is a gain a better estimate than P_{β}^4 . Each data point is computed from 10^6 MC samples.

become exact for large N . Indeed, we see that $\langle \tilde{r} \rangle$ start too low ($\langle \tilde{r} \rangle = 0.3937$) but then grows monotonously. However it is only at around $N \approx 100$ that $P_{4,4}^{N,N}$ comes closer than $P_{3,3}^{2,2}$. Similar monotonic improvement with N is also found for $\beta = 2$.

However, for $\beta = 1$, the surmise $P_{1,1}^{2,2}$ remains the best until $N \approx 15$. This situation is quite similar to that of the one-component surmises P_{β}^N . In that situation, there is an initial improvement for small N , which overshoots and finally improves again at $N \geq 100$ [18]. For clarity, this behavior is reproduced in Figure 4.

For the other surmises of the form $P_{\beta,\beta'}^{4-N,N}$ no numerical comparisons are done, as it is unclear that thermodynamic distributions they would approximate.

IV. ANALYTICAL RESULTS

In this section we summarize our analytical results. The main results is that of $P_{\beta,\beta}^{2,2}(r)$ but for completeness we also list more distributions. As the formulas are computer generated automatically, step by step derivations will not be shown, but intermediates results have been set aside by the algorithms,

At the moment memory restrains in prevent us from also computing $P_{\beta}^4(r)$ for higher values of β , but there is no conceptual problem in going further.

To keep this section more compact we use the following abbreviations

$$\begin{aligned}\delta &= r + 1 \\ \gamma &= r^2 + r + 1 \\ d_{443} &= 4r^2 + 4r + 3\end{aligned}\quad (8)$$

$$d_{344} = 3r^2 + 4r + 4 \quad (9)$$

$$T(r) = \tan^{-1} \left(\frac{r+2}{2\sqrt{2}\gamma} \right) \quad (9)$$

$$T\left(\frac{1}{r}\right) = \tan^{-1} \left(\frac{2r+1}{2\sqrt{2}\gamma} \right) \quad (10)$$

We also make use of the polynomials $F_{\beta}^{\bar{N}}(r), G_{\beta}^{\bar{N}}(r)$ and $E_{\beta}^{\bar{N}}(r)$. The first two polynomials are dual, such that $F_{\beta}^{\bar{N}}\left(\frac{1}{r}\right) r^{\deg(F_{\beta}^{\bar{N}})} = G_{\beta}^{\bar{N}}(r)$ whereas $E_{\beta}^{\bar{N}}\left(\frac{1}{r}\right) r^{\deg(E_{\beta}^{\bar{N}})} = E_{\beta}^{\bar{N}}(r)$ is self-dual.

A. One component mixtures

The one-component mixtures P_{β}^N for $N = 3$ where solved for arbitrary integer β in Ref. 17. In a subsequent work[18] they also computed the next order for $\beta = 1$. Using our method we can easily reproduce this result

$$P_1^4(r) = \frac{r\delta}{4\gamma^4} \left(\frac{F_1^4(r)}{d_{443}^{5/2}} + \frac{G_1^4(r)}{d_{344}^{5/2}} \right) \quad (11)$$

with the auxiliary polynomials

$$\begin{aligned}F_1^4(r) &= 512r^8 + 2048r^7 + 3768r^6 + 4136r^5 \\ &\quad + 2696r^4 + 888r^3 - 49r^2 - 145r - 30 \\ G_1^4(r) &= -30r^8 - 145r^7 - 49r^6 + 888r^5 + 2696r^4 \\ &\quad + 4136r^3 + 3768r^2 + 2048r + 512.\end{aligned}$$

Ideally we would like to also target larger values of both N and β but at present this requires improved algorithms.

B. Mixtures with independent level ($\beta = 0$)

We begin with listing mixtures containing uncorrelated eigenvalues ($\beta = 0$). The distribution for $N = 4$ independent eigenvalues are given by

$$P_0^4(r) = \frac{3}{2\pi\gamma} \left(2\sqrt{3} - \frac{2+r}{\sqrt{d_{344}}} - \frac{1+2r}{\sqrt{d_{443}}} \right). \quad (12)$$

Mixtures where one of the component only has one eigenvalue gives identical results to setting the $\beta = 0$ for that component, giving $P_{\beta,\alpha}^{2,1} = P_{\beta,0}^{2,1}$. The surmises for

not setup are thus given by

$$P_{1,0}^{2,1}(r) = \frac{3}{4} \frac{\delta}{\gamma^{3/2}} \quad (13)$$

$$P_{2,0}^{2,1}(r) = \frac{3\sqrt{3}}{2\pi\gamma} \quad (14)$$

$$P_{3,0}^{2,1}(r) = \frac{27(2r^3 + 3r^2 + 3r + 2)}{64\gamma^{5/2}} \quad (15)$$

$$P_{4,0}^{2,1}(r) = \frac{3\sqrt{3}}{2\pi\gamma}, \quad (16)$$

where we note that $P_{2,0}^{2,1} = P_{4,0}^{2,1}(r)$. For $N = 3$ the results are

$$P_{1,0}^{3,1}(r) = \frac{\delta^2}{\gamma^2} \frac{E_{1,1}^{3,1}(r)}{\sqrt{2\pi}d_{443}^2d_{344}^2} + \frac{(r^2 + 10r + 1)\delta}{4\pi\gamma^{5/2}} \left[\pi - T(r) - T\left(\frac{1}{r}\right) \right] \quad (17)$$

$$P_{2,0}^{3,1}(r) = \frac{\sqrt{3}E_{2,0}^{3,1}(r)}{2\pi\delta^4} - \frac{F_{2,0}^{3,1}(r)}{4\pi\delta^4d_{344}^{7/2}} - \frac{G_{2,0}^{3,1}(r)}{4\pi\delta^4d_{443}^{7/2}} \quad (18)$$

$$P_{0,3}^{1,3}(r) = \frac{3E_{0,3}^{1,3}(r)\delta}{224\pi\gamma^{11/2}} \left[\pi - T(r) - T\left(\frac{1}{r}\right) \right] + \frac{d^2\tilde{E}_{0,3}^{1,3}(r)}{280\sqrt{2\pi}\gamma^5d_{344}^5d_{443}^5} \quad (19)$$

with

$$\begin{aligned}E_{1,0}^{3,1}(r) &= 312r^8 + 708r^7 + 1142r^6 + 969r^5 \\ &\quad + 998r^4 + 969r^3 + 1142r^2 + 708r + 312.\end{aligned}$$

and

$$\begin{aligned}E_{2,0}^{3,1}(r) &= 4r^6 + 12r^5 + 51r^4 + 82r^3 + 51r^2 + 12r + 4 \\ F_{2,0}^{3,1}(r) &= -36r^{13} - 276r^{12} + 677r^{11} + 10816r^{10} \\ &\quad + 45017r^9 + 110550r^8 + 185820r^7 \\ &\quad + 225768r^6 + 201768r^5 + 131664r^4 \\ &\quad + 61248r^3 + 19456r^2 + 4160r + 640 \\ G_{2,0}^{3,1}(r) &= 640r^{13} + 4160r^{12} + 19456r^{11} + 61248r^{10} \\ &\quad + 131664r^9 + 201768r^8 + 225768r^7 \\ &\quad + 185820r^6 + 110550r^5 + 45017r^4 \\ &\quad + 10816r^3 + 677r^2 - 276r - 36.\end{aligned}$$

$$\begin{aligned}E_{0,3}^{1,3}(r) &= 44r^8 + 154r^7 + 175r^6 + 1476r^5 \\ &\quad + 2710r^4 + 1476r^3 + 175r^2 + 154r + 44\end{aligned}$$

$$\begin{aligned}
\tilde{E}_{0,3}^{1,3}(r) = & 133318656r^{26} + 1849393152r^{25} + 14056292352r^{24} + 71482931456r^{23} + 264844710656r^{22} \\
& + 748372542976r^{21} + 1652680538624r^{20} + 2871205333152r^{19} + 3859106493224r^{18} + 3743668969440r^{17} \\
& + 1905039479728r^{16} - 1307897322555r^{15} - 4438665127726r^{14} - 5742939216774r^{13} - 4438665127726r^{12} \\
& - 1307897322555r^{11} + 1905039479728r^{10} + 3743668969440r^9 + 3859106493224r^8 + 2871205333152r^7 \\
& + 1652680538624r^6 + 748372542976r^5 + 264844710656r^4 + 71482931456r^3 \\
& + 14056292352r^2 + 1849393152r + 133318656
\end{aligned}$$

The integrals needed to reach higher β include increasing amount of terms and are left for the future.

There are no surmises of the form $P_{\beta,0,0}^{N,1,1}$ since if several components have only one eigenvalue, they can be modeled as one single component with $\beta = 0$, giving $P_{\beta,0,0}^{N,1,1} = P_{\beta,0}^{N,2}$. Thus, the next set of surmises is $P_{\beta,0}^{2,2}$ given by

$$\begin{aligned}
P_{0,1}^{2,2}(r) = & \frac{-3\delta T(r) + T(\frac{1}{r}) + \pi}{4\pi} \frac{\gamma^{3/2}}{\gamma^{3/2}} \\
& + \frac{3}{\sqrt{2}\pi} \frac{6r^4 + 9r^3 + 14r^2 + 9r + 6}{\gamma d_{344} d_{443}} \quad (20)
\end{aligned}$$

$$P_{0,2}^{2,2}(r) = \frac{3\sqrt{3}}{\pi\gamma} - \frac{3}{2\pi\gamma} \left(\frac{r+2}{d_{344}^{1/2}} + \frac{2r+1}{d_{443}^{1/2}} \right) \quad (21)$$

$$\begin{aligned}
P_{0,3}^{2,2}(r) = & \frac{27}{64} \frac{2r^3 + 3r^2 + 3r + 2}{\gamma^{5/2}} \\
& - \frac{3}{32\pi} \frac{F_{0,3}^{2,2}(r)T(r) + G_{0,3}^{2,2}(r)T(\frac{1}{r})}{\gamma^{5/2}} \\
& + \frac{E_{0,3}^{2,2}}{4\sqrt{2}\pi\gamma^2 d_{344}^2 d_{443}^2} \quad (22)
\end{aligned}$$

$$P_{0,4}^{2,2}(r) = \frac{3\sqrt{3}}{\pi\gamma} - \frac{F_{0,4}^{2,2}(r)}{6\pi\gamma d_{344}^{5/2}} - \frac{G_{0,4}^{2,2}(r)}{6\pi\gamma d_{443}^{5/2}} \quad (23)$$

The auxiliary functions for $\beta = 3$ and $\beta = 4$ are given by

$$\begin{aligned}
F_{0,3}^{2,2}(r) = & 10r^3 + 15r^2 + 12r + 8 \\
G_{0,3}^{2,2}(r) = & 8r^3 + 12r^2 + 15r + 10 \\
E_{0,3}^{2,2}(r) = & 816r^{10} + 3960r^9 + 12012r^8 + 24290r^7 \\
& + 36876r^6 + 41927r^5 + 36876r^4 + 24290r^3 \\
& + 12012r^2 + 3960r + 816
\end{aligned}$$

and

$$\begin{aligned}
F_{0,4}^{2,2}(r) = & 69r^5 + 350r^4 + 788r^3 + 1032r^2 + 760r + 304 \\
G_{0,4}^{2,2}(r) = & 304r^5 + 760r^4 + 1032r^3 + 788r^2 + 350r + 69.
\end{aligned}$$

C. Equal β mixtures $P_{\beta,\beta}^{2,2}$

In this subsection we list the surmises that figure in the main text, and are on the form $P_{\beta,\beta}^{2,2}$. These are

$$P_{1,1}^{2,2}(r) = \frac{\delta}{4\gamma^2} \left(\frac{F_{1,1}^{2,2}(r)}{d_{443}^{3/2}} + r \frac{G_{1,1}^{2,2}(r)}{d_{344}^{3/2}} \right) \quad (24)$$

$$P_{2,2}^{2,2}(r) = \frac{3}{\pi\gamma} \left(\sqrt{3} - \frac{F_{2,2}^{2,2}(r)}{4d_{443}^{5/2}} - \frac{G_{2,2}^{2,2}(r)}{4d_{344}^{5/2}} \right). \quad (25)$$

$$P_{3,3}^{2,2}(r) = \frac{3\delta}{64\gamma^4} \left(\frac{F_{3,3}^{2,2}(r)}{d_{344}^{7/2}} + \frac{G_{3,3}^{2,2}(r)}{d_{443}^{7/2}} \right). \quad (26)$$

$$\begin{aligned}
P_{4,4}^{2,2}(r) = & \frac{1}{\gamma^4} \frac{3}{2\pi} \left(\frac{2E_{4,4}^{2,2}(r)}{3\sqrt{3}} - \frac{(2r+1)F_{4,4}^{2,2}(r)}{d_{443}^{9/2}} \right. \\
& \left. - \frac{(2+r)G_{4,4}^{2,2}(r)}{d_{344}^{9/2}} \right). \quad (27)
\end{aligned}$$

The auxiliary functions are given by

$$\begin{aligned}
F_{1,1}^{2,2}(r) = & 16r^3 + 34r^2 + 31r + 15 \\
G_{1,1}^{2,2}(r) = & 15r^3 + 31r^2 + 34r + 16,
\end{aligned}$$

$$\begin{aligned}
F_{2,2}^{2,2}(r) = & (2r+1) \left((4r^2 + 4r + 7)^2 - 7 \right) \\
G_{2,2}^{2,2}(r) = & (r+2) \left((7r^2 + 4r + 4)^2 - 7r^4 \right)
\end{aligned}$$

$$\begin{aligned}
F_{3,3}^{2,2}(r) = & 918r^{12} + 6120r^{11} + 22107r^{10} + 53227r^9 \\
& + 92358r^8 + 119122r^7 + 114220r^6 + 79416r^5 \\
& + 36816r^4 + 8528r^3 - 1248r^2 - 1408r - 256, \\
G_{3,3}^{2,2}(r) = & -256r^{12} - 1408r^{11} - 1248r^{10} + 8528r^9 \\
& + 36816r^8 + 79416r^7 + 114220r^6 + 119122r^5 \\
& + 92358r^4 + 53227r^3 + 22107r^2 + 6120r + 918.
\end{aligned}$$

$$\begin{aligned}
E_{4,4}^{2,2}(r) &= 11r^6 + 33r^5 + 39r^4 + 23r^3 + 39r^2 + 33r + 11 \\
F_{4,4}^{2,2}(r) &= 96r^{14} + 672r^{13} + 2144r^{12} + 4128r^{11} \\
&\quad + 6712r^{10} + 11736r^9 + 22172r^8 + 36224r^7 \\
&\quad + 46551r^6 + 45581r^5 + 33883r^4 + 18731r^3 \\
&\quad + 7467r^2 + 1953r + 279 \\
G_{4,4}^{2,2}(r) &= 279r^{14} + 1953r^{13} + 7467r^{12} + 18731r^{11} \\
&\quad + 33883r^{10} + 45581r^9 + 46551r^8 + 36224r^7 \\
&\quad + 22172r^6 + 11736r^5 + 6712r^4 + 4128r^3 \\
&\quad + 2144r^2 + 672r + 96.
\end{aligned}$$

D. Distributions with mixed β

Mixtures with 2+2 eigenvalues also admit a series of surmises with mixed values of beta. Below we list these 6 combinations for $1 \leq \beta \leq 4$:

Surmise $P_{1,2}^{2,2}(r)$:

$$\begin{aligned}
P_{1,2}^{2,2}(r) &= \frac{22r^3 + 53r^2 + 53r + 22}{32\gamma^{5/2}} \quad (28) \\
&\quad - \frac{F_{1,2}^{2,2}(r)T(r) + G_{1,2}^{2,2}(r)T\left(\frac{1}{r}\right)}{16\pi\gamma^{5/2}} \\
&\quad + \frac{E_{1,2}^{2,2}(r)}{2\sqrt{2}\pi\gamma^2 d_{344}^2 d_{443}^2}
\end{aligned}$$

$$\begin{aligned}
F_{1,2}^{2,2}(r) &= 2r^3 + 13r^2 + 40r + 20 \\
G_{1,2}^{2,2}(r) &= 20r^3 + 40r^2 + 13r + 2 \\
E_{1,2}^{2,2}(r) &= 384r^{10} + 2160r^9 + 6896r^8 + 14200r^7 \\
&\quad + 21616r^6 + 24559r^5 + 21616r^4 \\
&\quad + 14200r^3 + 6896r^2 + 2160r + 384.
\end{aligned}$$

Surmise $P_{1,3}^{2,2}(r)$:

$$P_{1,3}^{2,2}(r) = \frac{1}{8\gamma^3} \left(\frac{F_{1,3}^{2,2}(r)}{d_{344}^{5/2}} + \frac{G_{1,3}^{2,2}(r)}{d_{443}^{5/2}} \right) \quad (29)$$

$$\begin{aligned}
F_{1,3}^{2,2}(r) &= 96r^9 + 533r^8 + 1518r^7 + 2719r^6 \\
&\quad + 3306r^5 + 2748r^4 + 1488r^3 + 448r^2 + 24r - 16 \\
G_{1,3}^{2,2}(r) &= -16r^9 + 24r^8 + 448r^7 + 1488r^6 \\
&\quad + 2748r^5 + 3306r^4 + 2719r^3 + 1518r^2 + 533r + 96
\end{aligned}$$

Surmise $P_{1,4}^{2,2}(r)$:

$$\begin{aligned}
P_{1,4}^{2,2}(r) &= \frac{E_{1,4}^{2,2}(r)}{128\gamma^{7/2}} + \frac{F_{1,4}^{2,2}T(r) + G_{1,4}^{2,2}T\left(\frac{1}{r}\right)}{64\pi\gamma^{7/2}} \\
&\quad + \frac{\tilde{E}_{1,4}^{2,2}(r)}{48\sqrt{2}\pi\gamma^3 d_{344}^3 d_{443}^3} \quad (30)
\end{aligned}$$

$$\begin{aligned}
E_{1,4}^{2,2}(r) &= 78r^5 + 307r^4 + 566r^3 + 566r^2 + 307r + 78 \\
F_{1,4}^{2,2}(r) &= 6r^5 - 41r^4 - 238r^3 - 328r^2 - 266r - 84 \\
G_{1,4}^{2,2}(r) &= -84r^5 - 266r^4 - 328r^3 - 238r^2 - 41r + 6
\end{aligned}$$

$$\begin{aligned}
\tilde{E}_{1,4}^{2,2}(r) &= 113664r^{16} + 1046720r^{15} + 5063040r^{14} \\
&\quad + 16406704r^{13} + 39749568r^{12} + 75927300r^{11} \\
&\quad + 118307400r^{10} + 153231453r^9 + 166874784r^8 \\
&\quad + 153231453r^7 + 118307400r^6 + 75927300r^5 \\
&\quad + 39749568r^4 + 16406704r^3 + 5063040r^2 \\
&\quad + 1046720r + 113664
\end{aligned}$$

Surmise $P_{2,3}^{2,2}(r)$:

$$\begin{aligned}
P_{2,3}^{2,2}(r) &= \frac{9E_{2,3}^{2,2}(r)}{256\gamma^{7/2}} - \frac{3\left(F_{2,3}^{2,2}(r)T(r) + G_{2,3}^{2,2}(r)T\left(\frac{1}{r}\right)\right)}{128\pi\gamma^{7/2}} \\
&\quad + \frac{\tilde{E}_{2,3}^{2,2}(r)}{32\sqrt{2}\pi\gamma^3 d_{344}^3 d_{443}^3} \quad (31)
\end{aligned}$$

$$\begin{aligned}
E_{2,3}^{2,2}(r) &= 26r^5 + 65r^4 + 74r^3 + 74r^2 + 65r + 26 \\
F_{2,3}^{2,2}(r) &= 10r^5 + 25r^4 + 82r^3 + 140r^2 + 170r + 68 \\
G_{2,3}^{2,2}(r) &= 68r^5 + 170r^4 + 140r^3 + 82r^2 + 25r + 10 \\
\tilde{E}_{2,3}^{2,2}(r) &= 50688r^{16} + 464832r^{15} + 2619648r^{14} \\
&\quad + 10088176r^{13} + 28593440r^{12} + 62047380r^{11} \\
&\quad + 106098928r^{10} + 145418249r^9 + 161380392r^8 \\
&\quad + 145418249r^7 + 106098928r^6 + 62047380r^5 \\
&\quad + 28593440r^4 + 10088176r^3 + 2619648r^2 \\
&\quad + 464832r + 50688
\end{aligned}$$

Surmise $P_{2,4}^{2,2}(r)$:

$$P_{2,4}^{2,2}(r) = \frac{E_{2,4}^{2,2}(r)}{4\sqrt{3}\pi\gamma^4} - \frac{F_{2,4}^{2,2}(r)}{24\pi\gamma^4 d_{344}^{7/2}} - \frac{G_{2,4}^{2,2}(r)}{24\pi\gamma^4 d_{443}^{7/2}} \quad (32)$$

$$\begin{aligned}
E_{2,4}^{2,2}(r) &= 38r^6 + 114r^5 + 201r^4 + 212r^3 \\
&\quad + 201r^2 + 114r + 38 \\
F_{2,4}^{2,2}(r) &= 2682r^{13} + 20562r^{12} + 79123r^{11} + 200738r^{10} \\
&\quad + 368767r^9 + 518820r^8 + 574926r^7 + 516036r^6 \\
&\quad + 380856r^5 + 235584r^4 + 119856r^3 + 48416r^2 \\
&\quad + 13312r + 2048 \\
G_{2,4}^{2,2}(r) &= 2048r^{13} + 13312r^{12} + 48416r^{11} + 119856r^{10} \\
&\quad + 235584r^9 + 380856r^8 + 516036r^7 + 574926r^6 \\
&\quad + 518820r^5 + 368767r^4 + 200738r^3 + 79123r^2 \\
&\quad + 20562r + 2682
\end{aligned}$$

Surmise $P_{3,4}^{2,2}(r)$:

$$P_{3,4}^{2,2}(r) = \frac{E_{3,4}^{2,2}(r)}{1024\gamma^{9/2}} - \frac{F_{3,4}^{2,2}(r)T(r) + G_{3,4}^{2,2}(r)T(\frac{1}{r})}{512\pi\gamma^{9/2}} + \frac{\tilde{E}_{3,4}^{2,2}(r)}{384\sqrt{2}\pi\gamma^4 d_{443}^3 d_{443}^4} \quad (33)$$

$$E_{3,4}^{2,2}(r) = 934r^7 + 3269r^6 + 5775r^5 + 7977r^4 + 7977r^3 + 5775r^2 + 3269r + 934$$

$$F_{3,4}^{2,2}(r) = 2r^7 + 7r^6 + 795r^5 + 2826r^4 + 5151r^3 + 4980r^2 + 3262r + 932$$

$$G_{3,4}^{2,2}(r) = 932r^7 + 3262r^6 + 4980r^5 + 5151r^4 + 2826r^3 + 795r^2 + 7r + 2$$

$$\begin{aligned} \tilde{E}_{3,4}^{2,2}(r) &= \\ &= 10285056r^{22} + 126869760r^{21} + 832050432r^{20} \\ &+ 3751871232r^{19} + 12895150912r^{18} + 35584672928r^{17} \\ &+ 81305771632r^{16} + 156811861200r^{15} + 258577524828r^{14} \\ &+ 367643491941r^{13} + 453161735140r^{12} + 485718539552r^{11} \\ &+ 453161735140r^{10} + 367643491941r^9 + 258577524828r^8 \\ &+ 156811861200r^7 + 81305771632r^6 + 35584672928r^5 \\ &+ 12895150912r^4 + 3751871232r^3 + 832050432r^2 \\ &+ 126869760r + 10285056 \end{aligned}$$

V. SUMMARY AND DISCUSSION

This work used computer-generated algebra to compute gap ratios for all mixed Wigner surmises with $N = 3$ and $N = 4$ and $0 \geq \beta \geq 4$. Due to the memory constraints and evaluation times, we did not push the calculations to larger mixed ensembles. There is, however, no principal problem with looking at a larger number of eigenvalues. With improved algorithms, undoubtedly, larger ensembles of eigenvalue can be targeted.

We wish to point out that the numerical approach combined Julia and Mathematica code. The Julia controlled the flow of logic and algorithms, whereas Mathematica evaluated the algebraic expressions and performed certain integrals.

As for the analytical results, we hope that these will prove helpful as a simple diagnostic for mixed distributions. More elaborate diagnostics are also possible by considering higher-order statistics [21], and this work adds to that toolbox.

We find it a lucky coincidence that the $P_{3,3}^{2,2}$ surmise gives such a good approximation for the $2 \times \text{GSE}$ statistic, and it seems $P_{3,3}^{3,3}$ would be an almost perfect match. We leave it as an open question if the approximation is also suitable for higher-order correlations. While writing this manuscript, we became aware of the work in Ref. ? , where also the gap-ratio statistics of independent blocks were considered. However, that work had a slightly different focus, and thus the analytic results are somewhat different.

The reader will note that this work is only concerned with r -statistics and that no results for s -statistics are listed. The main reason for this is the problem that s -statistics has with unfolding, but there is also a technical aspect worth pointing out. For many of the surmises investigated here, the techniques to compute the r -statistic do not work to calculate the s -statistic. We thus leave these for future investigation.

ACKNOWLEDGMENTS

The author thanks Masud Haque and Lars Fritz for useful discussions. This work made use of Mathematica and the MathLink and MathLinkExtras packages for Julia.

This work is part of the D-ITP consortium, a program of the Netherlands Organisation for Scientific Research (NWO) that is funded by the Dutch Ministry of Education, Culture and Science (OCW).

-
- [1] M. V. Berry and M. Tabor, Proceedings of the Royal Society of London. A. Mathematical and Physical Sciences **356**, 375 (1977).
 - [2] O. Bohigas, M. J. Giannoni, and C. Schmit, Phys. Rev. Lett. **52**, 1 (1984).
 - [3] G. Casati, F. Valz-Gris, and I. Guarnieri, Lettere al Nuovo Cimento **28**, 279 (1980).
 - [4] M. V. Berry, Proceedings of the Royal Society of London. A. Mathematical and Physical Sciences **400**, 229 (1985).
 - [5] S. Gazit, F. F. Assaad, S. Sachdev, A. Vishwanath, and C. Wang, Proceedings of the National Academy of Sciences **115**, E6987 (2018).
 - [6] A. Chan, A. De Luca, and J. T. Chalker, Phys. Rev. Lett. **121**, 060601 (2018).
 - [7] V. Khemani, A. Lazarides, R. Moessner, and S. L. Sondhi, Phys. Rev. Lett. **116**, 250401 (2016).
 - [8] M. Fremling, C. Repellin, J.-M. Stéphan, N. Moran, J. Slingerland, and M. Haque, New Journal of Physics **20**, 103036 (2018).
 - [9] A. Milekhin, J. High Energ. Phys. **114** (2021).
 - [10] M. Fremling and L. Fritz, (2021), arXiv:2105.06119.
 - [11] M. Fremling, M. Haque, and L. Fritz, (2021), arXiv:2111.15215.
 - [12] M. Pretko, X. Chen, and Y. You, International Journal

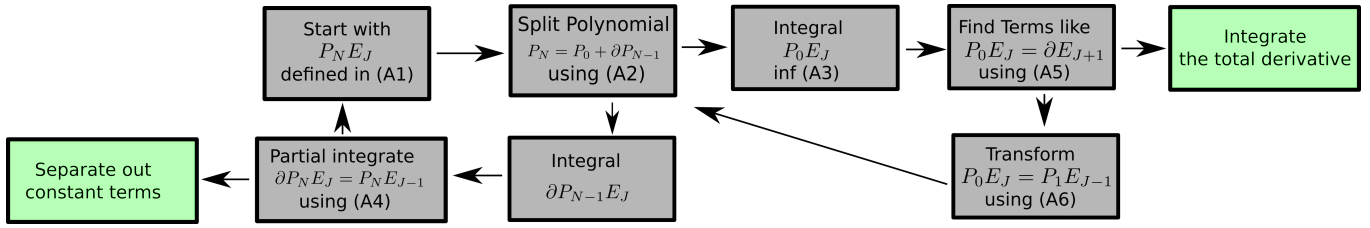


Figure 5. Flowchart of calculation described in Appendix A.

- of Modern Physics A **35**, 2030003 (2020).
- [13] P. Sala, T. Rakovszky, R. Verresen, M. Knap, and F. Pollmann, Phys. Rev. X **10**, 011047 (2020).
- [14] V. Khemani, M. Hermele, and R. Nandkishore, Phys. Rev. B **101**, 174204 (2020).
- [15] S. Moudgalya, A. Prem, R. Nandkishore, N. Regnault, and B. A. Bernevig, arXiv preprint arXiv:1910.14048 (2019).
- [16] V. Oganesyan and D. A. Huse, Phys. Rev. B **75**, 155111 (2007).
- [17] Y. Atas, E. Bogomolny, O. Giraud, and G. Roux, Physical review letters **110**, 084101 (2013).
- [18] Y. Atas, E. Bogomolny, O. Giraud, P. Vivo, and E. Vivo, Journal of Physics A: Mathematical and Theoretical **46**, 355204 (2013).
- [19] N. Chavda and V. Kota, Physics Letters A **377**, 3009 (2013).
- [20] U. T. Bhosale, S. H. Tekur, and M. Santhanam, Physical Review E **98**, 052133 (2018).
- [21] S. H. Tekur, U. T. Bhosale, and M. Santhanam, Physical Review B **98**, 104305 (2018).
- [22] S. H. Tekur, S. Kumar, and M. Santhanam, Physical Review E **97**, 062212 (2018).
- [23] S. H. Tekur and M. Santhanam, Physical Review Research **2**, 032063 (2020).
- [24] O. Giraud, N. Macé, É. Vernier, and F. Alet, Physical Review X **12**, 011006 (2022).
- [25] A. L. Corps and A. Relaño, Phys. Rev. E **101**, 022222 (2020).
- [26] Á. L. Corps and A. Relaño, Physical Review E **103**, 012208 (2021).
- [27] L. Sá, P. Ribeiro, and T. Prosen, Physical Review X **10**, 021019 (2020).
- [28] B. Dietz and F. Haake, Zeitschrift für Physik B Condensed Matter **80**, 153 (1990).

Appendix A: A recursive integration scheme

In this appendix, we describe schematically the steps needed to compute the distributions listed in section IV. In the course of computing the nested integral (7), we will encounter a few different types of specific integrals. The calculation relies on recursion and the flow is schematically illustrated in Figure 5. The first is the integral over the δ -function, which is trivial, and we will not further mention it.

The second typical integral is of the form

$$\int P_N E_J = \int_0^\infty dx F_N(x) e^{-f(x)} \prod_{j=1}^J \text{erf}(p_j(x)) \quad (\text{A1})$$

where $F_N(x)$ is a polynomial in x of degree N , $f(x)$ is a second order polynomial in x and $p_j(x)$ are a set of J first order polynomials in x .

The first step to integrate (A1) is to rewrite the first two factors of the integrand as

$$F_N(x) e^{-f(x)} = F_0 e^{-f(x)} + \frac{\partial}{\partial x} \left[F_{N-1}(x) e^{-f(x)} \right]. \quad (\text{A2})$$

Here F_0 is a constant and $F_{N-1}(x)$ is a polynomial one degree lower than $F_N(x)$. Schematically we have $P_N = P_0 + \partial P_{N-1}$. Inserting (A2) into (A1), one obtains two terms as

$$\int P_N E_J = \int P_0 E_J + \int (\partial P_{N-1}) E_J.$$

The first, $\int P_0 E_J$, has no polynomial part and is given by

$$\int P_0 E_J = F_0 \int_0^\infty dx e^{-f(x)} \prod_{j=1}^J \text{erf}(p_j(x)). \quad (\text{A3})$$

We leave this term as it is for the time being.

The second piece $\int (\partial P_{N-1}) E_J$, contains an explicit derivative and can be approached by partial integration as

$$\begin{aligned}
\int (\partial P_{N-1}) E_J &= \int_0^\infty dx \frac{\partial}{\partial x} \left[F_{N-1}(x) e^{-f(x)} \right] \prod_{j=1}^J \operatorname{erf}(p_j(x)) \\
&= \left[F_{N-1}(x) e^{-f(x)} \prod_{j=1}^J \operatorname{erf}(p_j(x)) \right]_0^\infty - \int_0^\infty dx \left[F_{N-1}(x) e^{-f(x)} \right] \frac{\partial}{\partial x} \left(\prod_{j=1}^J \operatorname{erf}(p_j(x)) \right).
\end{aligned} \tag{A4}$$

The first term can be evaluated directly, and the second term (after acting with the derivatives) is again of the form (A1), but now with $N \rightarrow N - 1$ and $J \rightarrow J - 1$. By recursion, which stops when $N = 0$, the only unintegrated terms left will be of the form $\int P_0 E_J$ given Eqn. (A3).

The integral $\int P_0 E_J$ is integrated in two steps. First we search for terms that can be combined to form products of erf-functions $\prod_{j=1}^{J+1} \operatorname{erf}(p_j(x))$. For this we use that

$$\frac{\partial}{\partial x} \prod_{j=1}^{J+1} \operatorname{erf}(p_j(x)) = \sum_{k=1}^{J+1} \left(\frac{\partial p_k}{\partial x} \right) e^{-p_k^2(x)} \prod_{k \neq j=1}^{J+1} \operatorname{erf}(p_j(x)) \tag{A5}$$

is a sum of terms on the form of $P_0 E_J$. If the total derivative $\partial(E_{J+1}) = P_0 E_J$ can be identified, the integral is trivially evaluated and put aside.

There may still be terms of the form $\int P_0 E_J$ that cannot be integrated by making use of (A5). To make progress, we represent the error function of x as an integral over an auxiliary variable t :

$$\operatorname{erf}(x) = x \sqrt{\frac{2}{\pi}} \int_0^1 dt e^{-x^2 t^2}. \tag{A6}$$

With this transformation we can represent $\int P_0 E_J$ as an integral on the form $\int P_1 E_{J-1}$ and repeat the steps following equation (A2), until all error functions have been integrated (or transformed away).

Using the auxiliary variables t , we can perform all the integrals, with the price that we now must integrate over the additional variables t_i at the end. Fortunately, the integrals that we consider in this work can always be performed with the help of Euler substitution.

Once all the computations have been performed, the total probability distribution is given by the sum of all the parts

$$P(r) = \frac{\sum_{k,\sigma} P_{k,\sigma}(r)}{\sum_{k,\sigma} Z_\sigma},$$

where Z_σ are the normalization constants of $P_\sigma(g)$.